**Fachtagung "Experimentelle Strömungsmechanik"**
4. – 6. September 2018, Rostock

# Experimental and numerical analyses of the texturisation process during high moisture extrusion cooking of soy protein

**E. Högg*, T. Horneber, C. Rauh**
Fachgebiet für Lebensmittelbiotechnologie und -prozesstechnik, TU Berlin,
Königin-Luise-Straße 22, 14195 Berlin
*E-Mail: e.hoegg@tu-berlin.de

Texturisation, High Moisture Extrusion Cooking (HMEC), CFD

## Abstract

During the last years, texturisation of vegetable proteins has been a major development in the food industry (Rhee et al. 1981). Plant-derived protein texturised using extruder technology is termed as texturate. These texturates have strong potential as an alternative to meat as they have a meat-like, fibrous texture and are produced by the High Moisture Extrusion Cooking (HMEC) process. Though the process, a twin-screw extruder with an elongated, double-walled cooling die is used (Brugger et al. 2017). In this cooling die the solidification of a plant-derived protein matrix takes place via a structuring process that has not yet been fully understood. To get an insight into the structure formation, *in-situ* measurements of pressure and temperature were carried out. Further numerical studies were conducted and unmeasurable parameters could be determined using inverse modeling. The results of the *in-situ* measurements of pressure and temperature are consistent with the results of the numerical studies and are also applicable to various die configurations. To characterize the structure of the texturates, textural analyses (slice shear force and tensile strength) were carried out. The textural analyses were used to determine a structuring index. Additionally a structuring coefficient of kinematic variables was determined in the numerical simulation.

## 1. Introduction

The extrusion cooking process at high moisture contents, so-called high moisture extrusion cooking (HMEC) process, offers considerable potential for the production of plant-derived meat analogues that resemble muscle meat. Due to mechanical and thermal stresses during the extrusion process proteins are altered in their native structure; denaturation and changes in their molecular structures occur (Liu and Hsieh 2007; Chen et al. 2011; Osen et al. 2015).
In the HMEC process the altered proteins are discharged through a long-drawn, double-walled cooling die which is attached at the end of the extruder barrel and prevents the protein matrix from expanding. In the cooling die a meat-like, fibrous structure is developed (Arêas 1992; Cheftel et al. 1992). The structuring process dependents on numerous factors, such as the composition of the raw material and the processes in the extruder barrel as well as in the cooling die and until now the whole process is not sufficiently understood.
To analyse the influence of the cooling die on the structuring process of a soy protein matrix, the configuration of the die was altered in width and height. Experimental studies were link with


Karlsruhe, Germany, ISBN 978-3-9816764-5-7

numerical simulation. Previous studies regarding this approach showed that the texturate preserves fluid-mechanical stresses in its layered structure due to the solidification in the cooling die and that the texturate shows a clearly defined, three-dimensional orientation, which is partly due to shear stresses during cooling (Högg et al. 2017).

## 2. Material and methods

### 2.1. Materials

The HMEC experiments were done with commercial soy protein concentrate (DuPont de Nemours (Germany) GmbH, Neu-Isenburg, Germany).

### 2.2. Experimental studies

#### 2.2.1. High moisture extrusion cooking

The HMEC experiments were performed as described in (Högg et al. 2017). However, the feed rate was set to $13\ \mathrm{kg\ h^{-1}}$ and $9\ \mathrm{kg\ h^{-1}}$ respectively. The other parameters were kept at constant value: screw speed of $400\ \mathrm{U\ min^{-1}}$, barrel temperature of $140\ ℃$ and moisture content of $60\ \%$ (wet basis).

#### 2.2.2. Cooling die

The cooling die at the extruder discharge was attached to the extruder by using a transition plate. To analyse the influence of the cooling die, three different configurations (r1 – r3) were applied differing in width and height; however, the length of the die was kept at a constant length of $250\ mm$ (see Table 1).

Table 1: List of three different configurations (r1, r2, r3) of the cooling die including transition plate to analyse the influence of the cooling die on the texturisation mechanism.

| **r1** | **length [mm]** | **width [mm]** | **height [mm]** |
|---|---|---|---|
| transition plate | 5 | 45.74 | 4.1 |
| cooling die | 250 | 60 | 9 |

| **r2** | **length [mm]** | **width [mm]** | **height [mm]** |
|---|---|---|---|
| transition plate | 5 | 45.00 | 4.1 |
| cooling die | 250 | 45 | 9 |

| **r3** | **length [mm]** | **width [mm]** | **height [mm]** |
|---|---|---|---|
| transition plate | 5 | 45.00 | 4.1 |
| cooling die | 250 | 45 | 6 |

The cooling temperature was set to a constant value of $40°C$ by an air-cooled thermostat (LAUDA DR. R. WOBSER GMBH & CO. KG, Lauda-Königshofen, Germany) for all three configurations and tap water functioned as coolant. The pressure gradient in the cooling die was measured using a melt pressure sensor MDT422 (Dynisco Instruments, LLC, Franklin, Massachusetts, USA) at the extruder outlet, directly before the cooling die inlet. Additionally, a temperature gradient was detected measuring the temperatures at a distance of $0.05\ \mathrm{m}$; $0.14\ \mathrm{m}$ and $0.23\ \mathrm{m}$ along the cooling die using thermocouples type J (Voltcraft, Wollerau, Switzerland)



Karlsruhe, Germany, ISBN 978-3-9816764-5-7

in all experiments (r1, r2, r3). The positions of the thermocouples were positioned $0.01\ \mathrm{m}$ outwards from the centre of the die.

### 2.3. Numerical studies

In the numerical experiments the solidification of the protein matrix in the cooling die was studied by using the commercial software ANSYS CFX (ANSYS, Inc., Canonsburg, Pennsylvania, USA). The inverse modeling was initially based on numerical simulations of the flow and temperature field and the boundary conditions were set as described in (Högg et al. 2017). Herschel-Bulkley Model with Arrhenius term was considered as the flow function with a yield stress $\tau_0$:

$$\mu = \frac{\tau_0}{\dot{\gamma}} + k\dot{\gamma}^{n-1}, \qquad k = k_0 \exp\left(\frac{A}{T}\right)$$

The yield stress $\tau_0$ was introduced in order to simulate a similar effect as a phase transition. The value for the yield stress was set to $\tau_0 = 1000\ Pa$ by inverse modeling. Rheological studies were done in the scope of the research project AiF 18727 N by the Institute of Process Engineering in Life Sciences Chair I: Food Process Engineering in Karlsruhe to determine the rheological properties of the protein matrix. Other material data have been determined experimentally or were taken out of the literature and are listed in Table 2. The material data were the same for all investigated die configurations.

Table 2: Material data of the soy protein matrix for the numerical simulation to study the solidification in a cooling die during HMEC.

| Parameter | | Value | Unit | Comment |
|---|---|---|---|---|
| moisture content | $X_W$ | 0.60 | - | experimental studies |
| molar mass | | 2516 | $kg\ mol^{-1}$ | Fang et al. 2013 |
| density | $\rho$ | 1078.59 | $kg\ m^{-3}$ | Calculated based on mass flow rate of $13\ kg\ h^{-1}$ and velocity of $0{,}0062\ m\ s^{-1}$ (experimental studies) |
| specific heat capacity | $c_p$ | 3467.70 | $J\ (kg\ K)^{-1}$ | at a reference temperature of $100\ °C$ $c_p = 4.1 * \mathrm{T} + 3057.7$ (experimental studies) |
| thermal conductivity | $\lambda$ | 0.4296 | $W(m\ K)^{-1}$ | $\lambda = -0.228 + 0.000249\rho + 1.304X_W - 0.926X_W^2$ (Wallapapan 1984) |
| flow index | $n$ | 0.15 | - | experimental studies[1] |
| consistency parameter | $k_0$ | 137.5 | - | experimental studies[1] |
| Arrhenius parameter | $A$ | 2020 | - | experimental studies[1] |

[1]Rheological studies were done in the scope of the research project AiF 18727 N by the Institute of Process Engineering in Life Sciences Chair I: Food Process Engineering in Karlsruhe


Karlsruhe, Germany, ISBN 978-3-9816764-5-7

Furthermore a slipping condition was defined as boundary condition at the wall:

$$u_{ws} = U_s \left( \frac{\tau_w - \tau_c}{\tau_n} \right), \qquad \tau_w > \tau_c$$

with

$$\begin{aligned} slip\ speed\ U_s &= \frac{\dot{m}}{\rho * A} && [mm\ s^{-1}] \\ normalizing\ stress\ \tau_n &= 1 && [Pa] \\ critical\ stress\ \tau_C &= 20\,000 && [Pa] \end{aligned}$$

The normalising stress $\tau_n$ was set to $1\ Pa$, whereby the value of critical stress $\tau_c = 20\,000\ Pa$ was assumed by inverse modeling.

### 2.4. Textural properties of texturates

#### 2.4.1. Experimental studies

The texture properties of the texturates were evaluated using a Zwick/Roell Z1.0 universal test machine (Zwick Roell, Ulm, Germany) according to the modified procedure of American Meat Science Association (2015), Chen et al. (2010) and Thiébaud et al. (1996). Samples were collected for each configuration setting and immediately stored in airtight plastic bags at $-20\ °C$. Prior to analysis, all samples were thawed at ambient temperature. A square shaped sample from the outer part of the texturate as well as from the center was cut using a knife blade with a diameter of $1\ mm$ thickness at a speed of $500\ mm\ min^{-1}$ and the cutting strength was recorded for the determination of the slice shear force (SSF). The samples were cut parallel ($F_l$) to the direction outflow from the cooling die. The measurements of tensile strength were carried out on the same Zwick/Roell Z1.0 universal test machine specially equipped with a lab-made system of two clamps to hold the sample. The tensile strength was measured parallel to the direction of texturate outflow at a speed of $200\ mm\ min^{-1}$ and the elastic modulus was recorded. All determinations were performed with at least 5 replicates.

#### 2.4.2. Numerical studies

In the numerical studies a structuring coefficient was determined calculating the coefficient of variation from kinematic variables. The total die volume was taken into consideration, expect of the first $0.01\ m$ of the cooling die inlet to not include the influence of the cross-section expansion between transition plate and cooling die.


Karlsruhe, Germany, ISBN 978-3-9816764-5-7

## 3. Results and discussion

During the experimental studies on the HMEC process various process parameters were determined that are listed in Table 3.

Table 3: List of the determined process data during experimental studies with different die configurations (r1, r2, r3) using the HMEC process

| **Process data of the experimental studies on the HMEC processs** | | | **r1** | **r2** | **r3** |
|---|---|---|---|---|---|
| temperature before cooling die inlet | $T_{\mathrm{in}}$ | °C | 116.4 | 115.6 | 120.5 |
| maximal temperature of product at die outlet | $T_{\mathrm{max,out}}$ | °C | 102.1 | 99.6 | 89.0 |
| average temperature of product at die outlet | $T_{\mathrm{avg,out}}$ | °C | 91.7 | 60.0 | 62.0 |
| mass flow rate | $\dot{m}$ | $\mathrm{kg\ h^{-1}}$ | 13 | 9 | 9 |
| temperature of cooling fluid before | $T_{\mathrm{CF,in}}$ | °C | 40.3 | 39.81 | 40.2 |
| temperature of cooling fluid after | $T_{CF,\mathrm{out}}$ | °C | 46.1 | 45.0 | 45.6 |
| heat transfer coefficient | $h$ | $\mathrm{W\ m^{-2}\ K^{-1}}$ | 639.51 | 2204.05 | 1612.68 |

The numerical studies are based on the measured process variables above. To assess non-measured material parameters, the numerical simulation is compared with experimental studies and adapted to experimental data.
During the experimental studies, *in-situ* measurements of pressure and temperature were carried out as mention in 2.2.2. The experimental data of the temperature measurements were compared with the numerical studies and are plotted in Figure 1.

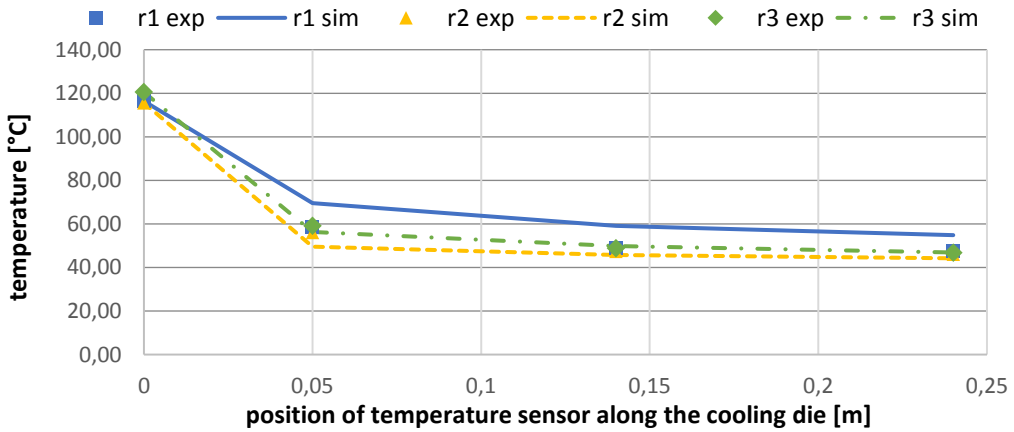


Figure 1: Comparing the *in-situ* measurements of temperature along the cooling die during high moisture extrusion cooking of the experimental studies (r1 exp; r2 exp; r3 exp) with the calculated temperature gradients along the cooling die in the numerical studies (r1 sim,; r2 sim; r3 sim). The three experiments (r1; r2; r3) differ in the die configuration (see Table 1).

The temperature drops rapidly in the first $0.05\ m$ of the cooling die and than adjusts to the set cooling die temperature of $40\ °C$ for all experiments (r1 – r3). The configuration setting with the narrowest cross-section (r3) shows the highest temperature drop. For the configuration setting with the widest cross-section (r1) the lowest temperature gardient is achieved and the results of the experimental studies are highly concordant with the results of the numerical studies (see Figure 1).

Additionally pressure gradients between die inlet and oulet were recorded and calculated in all experiments and are listed in Table 4. Further, the maximum product temperature at the die outlet as well as the average temperature of the product at die outlet were measured in the experimental studies and compared with the data of the numerical simulation (see Table 4).

Table 4: Comparing various process parameters of the experimental studies with the numerical studies. The cooling die configuration of r1 was 9 mm x 60 mm x 250 mm (height x width x length). The configuration of r2 was 9 mm x 45 mm x 250 mm and the configuration of r3 was 6 mm x 45 mm x 250 mm, respectively.

| **Process parameter of the HMEC experiments** | | **r1** | | **r2** | | **r3** | |
|---|---|---|---|---|---|---|---|
| | | *sim* | exp | *sim* | exp | *sim* | exp |
| Pressure loss in cooling die | $dp$ $MP$ | *1.48* | 1.51 | *1.52* | 1.67 | *2.03* | 2.17 |
| percentage deviation | | -1.7 % | | -9.0 % | | -6.6 % | |
| maximal temperature at die outlet | $T_{\mathrm{max,out}}$ °C | *81.62* | 92 | *70.86* | 60 | *67.81* | 62 |
| percentage deviation | | -11 % | | +18.1 % | | +9.4 % | |
| average temperature at die outlet | $T_{\mathrm{avg,out}}$ °C | *101.31* | 102.1 | *92.06* | 99.6 | *84.09* | 89 |
| percentage deviation | | -0,8 % | | -7.6 % | | -5.5 % | |

The maximal product temperatures at die outlet as well as the average temperatures at die outlet of the numerical studies are consistent with the data measured during the experimental studies. The maximal temperatures at die outlet differs by $\pm\,18\,\%$. The differences between experimental and numerical studies for the average temperature at die outlet are somewhat lower (between -$0.8$ and -$7.6\,\%$), whereby the temperatures at die outlet in the numerical simulation are underestimated. For the numerical studies the above-mentioned measured temperature at die inlet ($T_{\mathrm{in}}$) was set as boundary condition at the inlet (see Table 3).

Textural analyses were carried out to characterise the structure of the texturates. Therefore the samples taken out of the outer part ($o$) and center ($m$) were cut parallel ($F_l$) to the direction of outflow from the cooling die. The ratio of $\frac{F_{l,m}}{F_{l,o}}$ was calculated to determine a structuring index. Additionally the elastic modulus was calculated using measurements of tensile strength. In the numerical studies a structuring coefficient was determined calculating the coefficient of variation from kinematic variables. The results of the experimental and numerical studies are compared in Figure 2.



Karlsruhe, Germany, ISBN 978-3-9816764-5-7

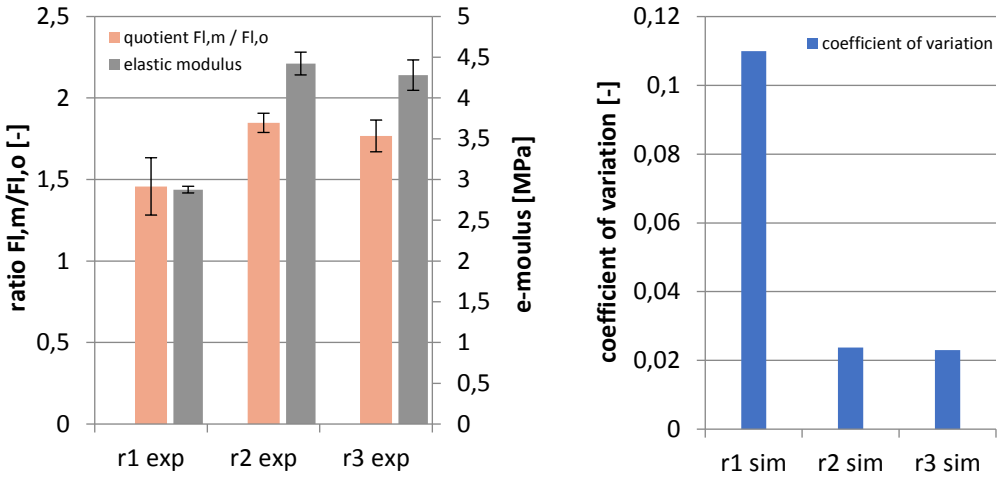


Figure 2: Comparison of the calculated structuring indices in the experimental (left) and numerical studies (right). Die configuration were as follows (height x width x length): r1: 9 mm x 60 mm x 250 mm; r2: 9 mm x 45 mm x 250 mm; r3: 6 mm x 45 mm x 250 mm.

On the left-hand side the results of the textural properties are shown. A dependency of the quotient $\frac{F_{l,m}}{F_{l,o}}$ on the die width is recognisable: the narrower the die width the higher the ratio $\frac{F_{l,m}}{F_{l,o}}$. Thus, the quotient $\frac{F_{l,m}}{F_{l,o}}$ increases from $1.46$ in the experiment r1 to $1.85$ in the experiment r2. However, the height of the die seems to have no significant influence on the quotient $\frac{F_{l,m}}{F_{l,o}}$ (see Figure 2, r2 exp and r3 exp). A similar effect is discernable in the results of the tensile strength: the elastic modulus increases with decreasing width. Therefore, the elastic modulus increases from $2.88\ MPa$ (r1 exp) to $4.42\ MPa$ (r2 exp). The increase in tensile strength and in the quotient $\frac{F_{l,m}}{F_{l,o}}$ due to the decrease in width can be explained by the developed flow profiles. The outer part of all texturates shows a pronounced profile. However, the profile gets flatten towards the center by increasing the die width (see Figure 3).

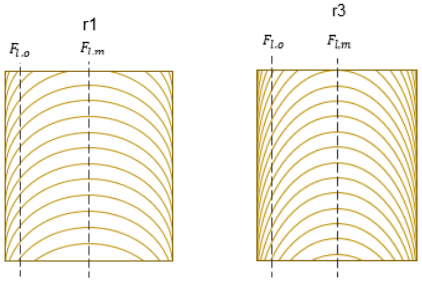


Figure 3: Draft of the developed flow profiles in the experiment r1 (left) and in the experiment r3 (right). The dotted lines mark the positions of the cuts in the analysis of shear slice force.

The complement to these analyses is the calculation of coefficient of variations (CV) from kinematic variables in the numerical studies. Experiment r2 und r3 show similar ratios und tensile strengths that can be also seen in the numerical studies (similar CVs). For the experiment r1 the elastic modulus as well as the ratio $\frac{F_{l,m}}{F_{l,o}}$ is lower and the calculated value of CV is higher. Therefore, different simulations can be compared regarding the degree of structuring using the calculated CV (high CV, poorly structured; lower CV, well structured).

In further studies, these results will be validated with other CVs from numerical simulations and, if necessary, further dimensionless parameters from kinematic variables will be used.


## Acknowledgements

This research project was supported by the German Ministry of Economics and Energy (via AiF) and FEI (Forschungskreis der Ernährungsindustrie e.V., Bonn) in the scope of project AiF 18727 N.


## Literature


American Meat Science Association (2015): Research Guidelines for Cookery, Sensory Evaluation, and Instrumental Tenderness Measurements of Meat.

Arêas, J. A. (1992): Extrusion of food proteins. In: *Critical reviews in food science and nutrition* 32 (4), S. 365–392. DOI: 10.1080/10408399209527604.

Brugger, C.; Dellemann, J. P.; Petry, C.; Laporte, M.; Müller, N.; Windhab, E. J. (2017): Next Generation Texturized Vegetable Proteins. In: food Marketing & Technology, S. 20–24.

Cheftel, J. C.; Kitagawa, M.; Quéguiner, C. (1992): New protein texturization processes by extrusion cooking at high moisture levels. In: *Food Reviews International* 8 (2), S. 235–275. DOI: 10.1080/87559129209540940.

Chen, Feng Liang; Wei, Yi Min; Zhang, Bo (2011): Chemicial cross-linking and molecular aggregation of soybean protein during extrusion cooking at low and high moisture content. In: *LWT - Food Science and Technology* 44 (4), S. 957–962. DOI: 10.1016/j.lwt.2010.12.008.

Chen, Feng Liang; Wei, Yi Min; Zhang, Bo; Ojokoh, Anthony Okhonlaye (2010): System parameters and product properties response of soybean protein extruded at wide moisture range. In: *Journal of Food Engineering* 96 (2), S. 208–213. DOI: 10.1016/j.jfoodeng.2009.07.014.

Högg E., Horneber T., Rauh C. (2017): Experimental and numerical analyses of the texturisation process of a viscoelastic protein matrix in a cooling die after high moisture extrusion cooking. In: Ruck B., Gromke C., Leder A., Dopheide D. (Hg.): 25. GALA-Fachtagung „Experimentelle Strömungsmechanik“. 5.-7. September 2017, Karlsruhe. Deutsche Gesellschaft für Laser-Anemometrie, 42-1 - 42-9.

Liu, Ke Shun; Hsieh, Fu-Hung (2007): Protein–Protein Interactions in High Moisture-Extruded Meat Analogs and Heat-Induced Soy Protein Gels. In: *J Amer Oil Chem Soc* 84 (8), S. 741–748. DOI: 10.1007/s11746-007-1095-8.

Osen, Raffael; Toelstede, Simone; Eisner, Peter; Schweiggert-Weisz, Ute (2015): Effect of high moisture extrusion cooking on protein-protein interactions of pea (Pisum sativum L.) protein isolates. In: *Int J Food Sci Technol* 50 (6), S. 1390–1396. DOI: 10.1111/ijfs.12783.

Rhee, K. C.; Kuo, C. K.; Lusas, E. W. (1981.): Texturization. In: *ACS Symposium Series; American Chemical Society* 147, S. 51–88. DOI: 10.1021/bk-1981-0147.ch004.

Thiébaud, Maryse; Dumay, Eliane; Cheftel, Jean Claude (1996): Influence of Process Variables on the Characteristics of a High Moisture Fish Soy Protein Mix Texturized by Extrusion Cooking. In: *LWT - Food Science and Technology* 29 (5-6), S. 526–535. DOI: 10.1006/fstl.1996.0080.